

Localized basis sets for unbound electrons in nanoelectronics

D. Soriano,^{1,*} D. Jacob,^{1,2,†} and J. J. Palacios^{1,‡}

¹*Departamento de Física Aplicada, Universidad de Alicante, San Vicente del Raspeig, Alicante 03690, Spain*

²*Department of Physics and Astronomy, Rutgers University, Piscataway NJ 08904 USA*

(Dated: November 29, 2018)

It is shown how unbound electron wave functions can be expanded in a suitably chosen localized basis sets for any desired range of energies. In particular, we focus on the use of gaussian basis sets, commonly used in first-principles codes. The possible usefulness of these basis sets in a first-principles description of field emission or scanning tunneling microscopy at large bias is illustrated by studying a simpler related phenomenon: The lifetime of an electron in a H atom subjected to a strong electric field.

I. INTRODUCTION

The theoretical description of the field emission (FE) mechanism has been traditionally based on the Wentzel-Kramers-Brillouin (WKB) approximation and simple band-structure models for the emitting tips¹. Research on field-emitting graphitic compounds has attracted much attention ever since its first observation in carbon nanotubes (CNT's) by de Heer et al.². Because of their high aspect ratio as well as mechanical and chemical stability, carbon nanotubes (CNT's) are regarded as potential materials for field emitters and this has been experimentally demonstrated in recent years^{3,4,5}. The electronic structure of CNT's and other graphitic materials strongly depends on details at the atomic level and not only on the overall shape. Therefore, an atomistic description of the emission process in these materials is pertinent. In this regard, tight-binding⁶, static density functional theory (DFT)^{7,8,9}, or time-dependent density functional theory (TDDFT)^{10,11} calculations have been able to explore the theoretical possibilities of some graphitic compounds as field emitters.

In the last decade a great deal of work has also been devoted to master electronic transport at the nanoscale. From a computational viewpoint the development of *ab initio* codes for quantum transport calculations has revolutionized the field, since, for the first time, reliable predictions are possible for the resistance of nanoscale objects when a current is driven through^{12,13,14,15,16}. Many of these codes are based on the non-equilibrium Green's function formalism (NEGF) which, in its most common implementation, requires the use of localized basis sets. This is an important drawback which hampers the straightforward applicability of these codes to describe FE processes where electron wave functions are unbound and extend into the vacuum.

A precise description of extended wave functions is also important when the electron transport takes place between electrodes or metallic tips that are significantly separated from each other. This is typically the case in scanning tunneling microscopy experiments where the metallic tip is several Å away from the surface and the electron current becomes a tunneling current. When one goes from the contact regime to the tunneling regime the

vacuum region becomes so wide that diffuse functions centered on the tip and the surface atoms cannot describe this region properly. Care must be taken complementing the basis set away from the tip and substrate¹⁷ for typical tip-surface distances. This is particularly important when a large voltage is applied between tip and sample which can affect the shape of the tunneling barrier to the point that electrons are emitted into the vacuum before reaching the substrate¹⁸.

In this report we examine the possibilities and limitations behind the use of localized atomic basis sets for the numerical description of free or unbound electrons. We are interested in the further implementation of these basis sets within our first-principles quantum transport package ALACANT (Alicante Ab initio Computation Applied to Nanotransport)^{13,14,19,20} which interfaces GAUSSIAN03²¹ or CRYSTAL²² packages. This is why we focus on the use of non-orthogonal gaussian-type functions. In Sec. II we present a detailed analysis of the completeness of gaussian basis sets in one dimension within a desired range of energies. In Sec. III we generalize the analysis to three-dimensional gaussian wave functions. In Sec. IV, as a simple illustration, we compute the lifetime of an electron in the $2s$ state of an H atom in the presence of an electric field using an appropriate basis set and compare with analytical calculations. Section V presents the conclusions.

II. BASIC THEORETICAL CONSIDERATIONS IN ONE DIMENSION

We consider first a one-dimensional free electron system described by the kinetic energy Hamiltonian $\hat{T}_x = \frac{1}{2} \frac{d^2}{dx^2}$. Here and in the following we use atomic units (A.U.) where the electron mass is set to one. The eigenstates are thus propagating waves which in the coordinate representation are given by $\psi_k(x) \propto \exp[ikx]$ with a real wavevector k and an energy dispersion given by

$$E(k) = \frac{k^2}{2}. \quad (1)$$

We want to describe free propagating waves with a basis set of localized atomic orbitals. As mentioned in the

introduction, we focus on the case of gaussian-type functions which are employed by many first-principles codes. In one dimension (1D) a gaussian-type function is given by:

$$\phi(x) = \sqrt{2\alpha/\pi} \exp[-\alpha x^2]. \quad (2)$$

We now place an infinite number of gaussian orbitals on a regular one-dimensional grid with lattice spacing a , and define the ket vector $|\phi_n\rangle$ corresponding to the gaussian wavefunction localized at grid point $x_n = na \vec{e}_x$ by $\langle x|\phi_n\rangle = \phi(x - na)$. The overlap integral between two gaussian orbitals on the grid separated by a distance na is thus given by

$$s(na) := \langle \phi|\phi_n\rangle = \exp[-\alpha(na)^2/2], \quad (3)$$

For the kinetic energy integral between gaussian orbitals separated by a distance na we have

$$\begin{aligned} t(na) &:= \langle \phi|\hat{T}_x|\phi_n\rangle = -\frac{1}{2}\langle \phi|\hat{p}^2|\phi_n\rangle \\ &= \frac{\alpha}{2}(1 - \alpha(na)^2) \exp[-\alpha(na)^2/2]. \end{aligned} \quad (4)$$

In this discrete basis set, the kinetic energy Hamiltonian \hat{T}_x can be diagonalized by transforming to Bloch states²³:

$$|\varphi_k\rangle = \sum_{n=-\infty}^{\infty} \exp[ikna] |\phi_n\rangle \Rightarrow \hat{T}_x|\varphi_k\rangle = \epsilon(k)|\varphi_k\rangle \quad (5)$$

Multiplying the eigenvalue equation by $\langle \phi|$ from the left and resolving for $\epsilon(k)$, the following dispersion relation is obtained:

$$\epsilon(k) = \frac{\langle \phi|\hat{T}_x|\varphi_k\rangle}{\langle \phi|\varphi_k\rangle} = \frac{\sum_{n=-\infty}^{\infty} \exp[ikna] t(na)}{\sum_{n=-\infty}^{\infty} \exp[ikna] s(na)}. \quad (6)$$

Obviously, the finer the grid, i.e. the smaller a , the better the dispersion relation must approach that of free electrons. In fact, in the limit of $a \rightarrow 0$, the expression (6) can be summed to yield the exact dispersion relation $E(k)$ independent of the gaussian exponent α (see Appendix):

$$\lim_{a \rightarrow 0} \epsilon(k) = \frac{\int dx t(x) \exp[ikx]}{\int dx s(x) \exp[ikx]} = \frac{k^2}{2} \equiv E(k). \quad (7)$$

Of course, this is somewhat trivial in reality since on an infinitely fine grid any orbital must expand the entire Hilbert space. A text-book choice in this limit is a basis of delta functions (Dirac basis), which is obtained from the gaussian functions by taking $\alpha \rightarrow \infty$:

$$\lim_{\alpha \rightarrow \infty} \sqrt{\frac{2\alpha}{\pi}} \exp[-\alpha(x - na)^2] = \delta(x - na). \quad (8)$$

However, for all practical purposes a finite grid parameter $a > 0$ must be set. Our aim now is to find an optimal α for a given a . Note, that the "atomistic" description always yields a finite maximal k -vector –the Brillouin zone

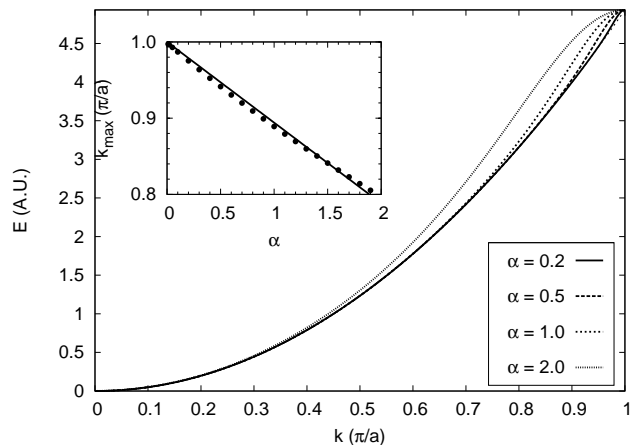


FIG. 1: Energy dispersions $\epsilon(k)$ for $a = 1$ A.U. and for different values of α . The inset shows the maximal k -value k_{\max} calculated from the inflection point of the energy dispersion $\epsilon(k)$ as explained in the text. The points have been calculated from individual dispersion curves while the line is a linear fit $k_{\max}(\alpha) = \pi/a - c \cdot \alpha$ to these points; $c \approx 0.33$ A.U..

(BZ) boundary $k_{\text{BZ}} = \pi/a$ – in contrast to truly free electrons where k is unbound. Fig. 1 shows the calculated dispersion $\epsilon(k)$ for fixed lattice parameter ($a = 1$ A.U.) and for different values of α . We see that in general the approximation works very well for smaller k -values, i.e. near the BZ center, but becomes worse towards the BZ boundary where the dispersion relation flattens out. Furthermore, the approximation is better, i.e. valid for a bigger range of k 's, the smaller α , i.e. the more diffuse the Gaussian function. However, it is already remarkably good for relatively large values of α . For instance, for $\alpha = 1$, $\epsilon(k)$ is a good approximation for k -values up to 70% of the theoretical upper limit k_{BZ} . This can also be seen from the effective mass $m^*(k) = (d^2\epsilon/dk^2)^{-1}$ calculated numerically from the dispersion relation $\epsilon(k)$, and shown in Fig. 2. The smaller α , the better does the effective mass m^* approximate the constant mass of truly free electrons ($m_e = 1$).

This suggests that $\epsilon(k) \rightarrow E(k)$ for $\alpha \rightarrow 0$ for $k \leq k_{\text{BZ}}$, so that the optimal exponent α would be zero. Of course, setting $\alpha = 0$ is numerically not feasible. In fact, in most quantum chemistry codes the gaussian exponents α cannot be chosen arbitrarily small for computational reasons. On the other hand, as can be seen from Fig. 1, the approximation is already quite good for reasonable values of α if we limit the range of wavevectors k to some k_{\max} smaller than the theoretical upper limit k_{BZ} . Since the slope of the real free-electron dispersion increases linearly with k , $dE/dk = k$, we define k_{\max} as the k -vector where the slope of the approximate energy dispersion $\epsilon(k)$ starts to decrease, i.e. at the inflection point of $\epsilon(k)$: $d^2\epsilon/dk^2(k_{\max}) \stackrel{!}{=} 0$. Clearly, at this point the effective mass $m^* = (d^2\epsilon/dk^2)^{-1}$ becomes infinite, so that our approximation is not valid any longer.²⁴ As

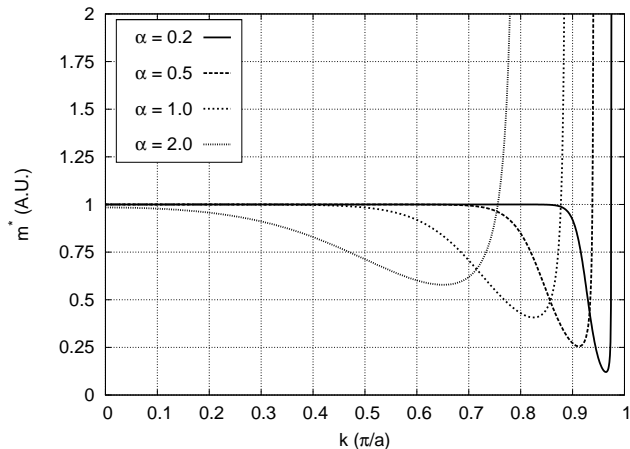


FIG. 2: Effective mass $m^*(k) = (d^2\epsilon/dk^2)^{-1}$ for $a = 1\text{A.U.}$ and for different values of α .

can be seen from the inset in Fig. 1, the thus calculated k_{\max} can be fitted very well by a linear function of the gaussian exponent α that approaches the BZ boundary $k_{\text{BZ}} = \pi/a$ for $\alpha \rightarrow 0$.

How does k_{\max} depend on the lattice parameter a ? Suppose that for a given lattice parameter a_0 and exponent α_0 we obtain a maximal range k_{\max}^0 . Thus we have:

$$\epsilon_{a_0, \alpha_0}(k_0) \approx \frac{k_0^2}{2} \text{ for all } k_0 \leq k_{\max}^0.$$

If we now alter the lattice spacing a and simultaneously scale α as $\alpha(a) = \alpha_0(a_0/a)^2$ and k as $k(a) = k_0(a_0/a)$ it is straightforward to show that the energy dispersion is essentially unchanged apart from an overall factor of $(a_0/a)^2$:

$$\epsilon_{a, \alpha}(k) = \left(\frac{a_0}{a}\right)^2 \epsilon_{a_0, \alpha_0}(k_0) \approx \left(\frac{a_0}{a}\right)^2 \frac{k_0^2}{2} = \frac{k^2}{2}$$

Thus $\epsilon_{a, \alpha}(k) = k^2/2$ for all k with $(a/a_0)k = k_0 \leq k_{\max}^0$, i.e. for all k with $k \leq (a_0/a)k_{\max}^0 \equiv k_{\max}$. Therefore k_{\max} scales exactly as the theoretical limit $k_{\text{BZ}} = \pi/a$ like $1/a$ with the lattice parameter a if we simultaneously scale the exponent α as $1/a^2$: $k_{\max}(a) = (a_0/a)k_{\max}^0$.

III. THREE-DIMENSIONAL GAUSSIAN FUNCTIONS

In three dimensions a gaussian wavefunction is given by

$$\Phi(\vec{r}) = (2\alpha/\pi)^{3/2} \exp[-\alpha \vec{r}^2] = \phi(x)\phi(y)\phi(z). \quad (9)$$

Again, we place the three-dimensional (3D) gaussian functions on a regular 1D grid along the x-axis with lattice spacing a , and define the ket vector $|\Phi_n\rangle$ corresponding to the gaussian function localized at grid point

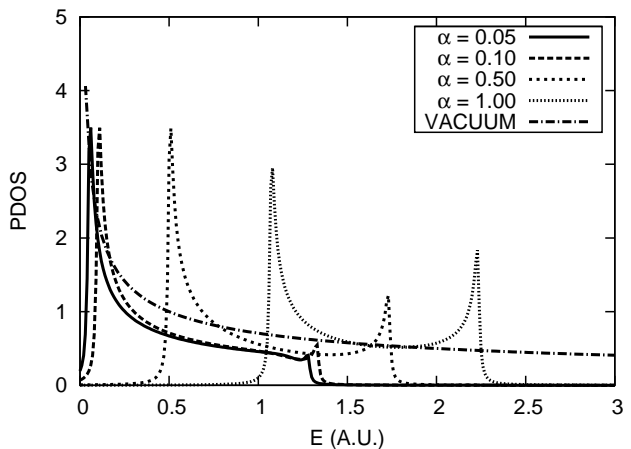


FIG. 3: DOS projected onto a bulk site i (PDOS) of a finite ($N=2001$) chain of gaussian functions for different values of the gaussian exponent, α , together with the DOS for free electrons moving in one dimension.

$\vec{r}_n = na\vec{e}_x$ by:

$$\langle \vec{r} | \Phi_n \rangle = \Phi(\vec{r} - \vec{r}_n) = \phi(x - na)\phi(y)\phi(z) \quad (10)$$

Now there is an additional contribution to the kinetic energy integral from the two directions (y and z) perpendicular to the direction (x) of the 1D grid:

$$\begin{aligned} t_{3D}(na) &:= \langle \Phi | (\hat{T}_x + \hat{T}_y + \hat{T}_z) | \Phi_n \rangle \\ &= \langle \phi | \hat{T} | \phi_{na} \rangle \langle \phi | \phi \rangle^2 + 2 \times \langle \phi | \phi_{na} \rangle \langle \phi | \phi \rangle \langle \phi | \hat{T} | \phi \rangle \\ &= t(na) + 2 \times s(na) \times t(0) \\ &= t(na) + \alpha s(na). \end{aligned} \quad (11)$$

Then, using Bloch's theorem we obtain the corresponding dispersion relation for 3D gaussian functions which differs from the analogous expression for 1D gaussian functions (6) only by a constant energy shift:

$$\epsilon_{3D}(k) = \alpha + \frac{\sum_{n=-\infty}^{\infty} t(na) \exp[ikna]}{\sum_{n=-\infty}^{\infty} s(na) \exp[ikna]}. \quad (12)$$

The constant energy shift α is due to the lateral confinement of the electrons to the region defined by the gaussian-shaped wavefunctions. Obviously, this confinement is eliminated by letting $\alpha \rightarrow 0$, i.e. by increasing the diffuseness of the gaussian orbitals and thus letting the lateral wavefunction $\phi(y) \times \phi(z)$ become a free electron wave with wavevector zero ($k_y = k_z = 0$). However, as said before, in most quantum chemistry packages the gaussian exponents cannot become arbitrarily small for computational reasons. Thus when the artificial offset needs to be reduced beyond the computational limit for the exponents, one has to reduce the lateral confinement of the electrons by extending the vacuum basis set with gaussian wavefunctions along the other two dimensions.

To analyze the density of states (DOS), we define the retarded Green's function in our non-orthogonal basis set

as (for details see e.g refs. 20,25)

$$\tilde{G}(E) = [(E + i\delta)S - T]^{-1}, \quad (13)$$

where δ is an infinitesimal quantity, S is the overlap matrix, and T is the 3D kinetic energy Hamiltonian represented in the non-orthogonal gaussian basis set. The integral over the total DOS, $\rho(E)$, must be equal to the number of basis functions, N , in our system.

$$N = \int_{-\infty}^{\infty} dE \rho(E) = -\frac{1}{\pi} \text{Im} \int_{-\infty}^{\infty} dE \text{Tr}[\tilde{G}(E)S] \quad (14)$$

In Fig. 3 we plot the DOS of a finite chain of $N = 2001$ gaussian functions projected (PDOS) on a bulk site i , i.e. $-\frac{1}{\pi} \text{Im}[\tilde{G}(E)S]_{i,i}$, for four values of the gaussian exponent α and a fixed grid parameter of $a = 2$ A.U.. The Green's function for an infinite system can be computed without difficulty²⁰. We prefer, nevertheless, to present results for finite systems here since these are the ones employed in the next section. Obviously, no differences should be expected for large enough systems. As discussed above, there is an unwanted contribution to the kinetic energy coming from the confinement in the two directions perpendicular to the direction of the atomic chain. This opens a gap in the PDOS close to zero energy which disappears as the exponent, and thus the lateral confinement, decreases. For values of the exponent $0.05 \leq \alpha \leq 0.1$ the PDOS already resembles that of free 1D electrons for energy values from 0.0 to 1.25 A.U.. The small but still visible gap in the PDOS at zero energy due to the residual lateral confinement can be eliminated by letting $\alpha \rightarrow 0$, but, as already mentioned, numerical limitations inherent to most computational packages do not recommend to do this. This already mentioned possibility of increasing the cross section of the chain by adding functions laterally will be explored in the future.

IV. IONIZATION OF THE $2s$ STATE OF THE HYDROGEN ATOM

In order to test the use of gaussian basis sets in realistic FE calculations, we have studied the ionization probability of the first excited state, $2s$, of the hydrogen atom in the presence of an electric field. For simplicity's sake, we have not included the $2p$ orbitals, although hybridization with them should be taken into account in a more realistic description of this problem. The calculations have been performed using the GAUSSIAN03 *ab initio* package as a complementary test for situations when the use of standard *ab initio* packages is convenient or necessary. The $2s$ orbital is coupled to two semi-infinite chains of gaussian functions representing the vacuum along the direction of the applied electric field as shown in Fig. 4. The straightforward use of GAUSSIAN03 forces us to work with finite vacuum chains as the one analyzed in the previous section. The results presented below have been



FIG. 4: One dimensional model where a central $2s$ orbital of a hydrogen atom is connected to semi-infinite chains of gaussian functions on both sides representing the vacuum. The electric field is applied along the chain direction.

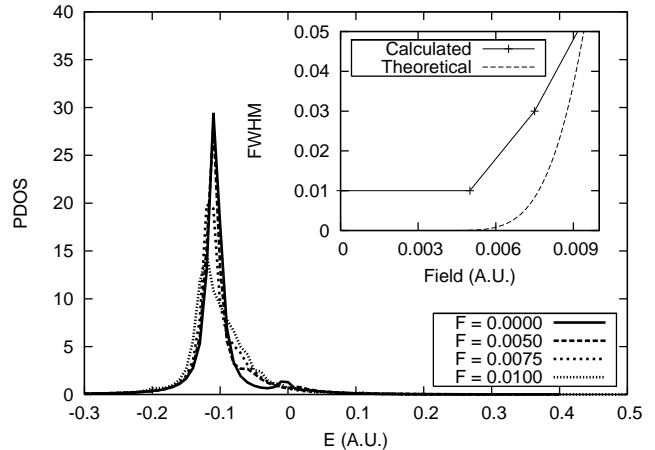


FIG. 5: Density of states projected on the $2s$ state of the hydrogen atom for different values of the applied electric field. In the inset the field dependence of the peak width is depicted and compared with the theoretical one (dotted line).

converged in the length of the lateral chains ($N = 1000$) so that no finite size effects can be appreciated.

The lifetime of the $2s$ state in the presence of an electric field can be extracted from the PDOS,

$$\rho_{2s}(E) = -\frac{1}{\pi} \text{Im}[\tilde{G}(E)S]_{2s,2s}. \quad (15)$$

The grid parameter and exponent for the two chains have been set to 1.0 \AA (~ 2 A.U.) and 0.07 A.U., respectively. The distance between the hydrogen atom and both vacuum chains has been fixed to 5.0 \AA (~ 10 A.U.) to optimize the hybridization between the vacuum states and the $2s$ state of the hydrogen atom. The $2s$ atomic orbital is modeled by the corresponding STO-6G basis function implemented in GAUSSIAN03 and the vacuum orbitals were implemented using ghost atoms. Care has been taken to remove the electron in the GAUSSIAN03 input file, reducing thus the calculation to a simple non-interacting problem.

The resonance width of the $2s$ orbital has been computed (see Fig. 5) and compared to the theoretical one²⁶ for some values of the electric field F (see inset in Fig.5). A finite value of δ (or fictitious width) is included to smear out the computed PDOS. This is why our results for the resonance width do not reach zero for zero applied field (see inset in Fig.5). As it would be expected the computed resonance width Γ_{2s} for the $2s$ state of the hydrogen atom is well approximated by the quasi-classical

theory:

$$\Gamma_{2s}(F) = \frac{1}{32F^2} \exp\left(-\frac{1}{12F}\right) \quad (16)$$

Considering the simplifications in our calculation which has been restricted to one dimension and that little care has been taken in completing the basis set around the $2s$ orbital, the results are qualitatively similar to the theoretical ones. This illustrates that localized basis sets, when appropriately chosen, can be used to represent unbound electron wavefunctions which are required to describe FE phenomena or high-bias STM.

V. CONCLUSIONS

In this work we have shown the possibility of representing unbound electron states using localized gaussian-type functions as a basis set. Although plane waves are a more natural basis for unbound electrons, localized basis sets have to be employed for the computation of field emission phenomena in the framework of many commonly used ab initio quantum transport packages such as ALACANT. In addition these basis sets provide a more natural way of quantifying local atomic properties when needed. As an illustration we have studied numerically the lifetime of an electron in the $2s$ orbital of the H atom in the presence of an electric field with the help of the GAUSSIAN03 package.

VI. ACKNOWLEDGEMENTS

This work has been funded by Spanish MEC under Grants Nos. MAT2007-65487 and CSD2007-00010, and by Generalitat Valenciana under Grant No. ACOMP07/054. D.S. acknowledges financial support from Instituto de Cultura Juan Gil-Albert. D.J. acknowledges financial support from the Spanish MEC under Grant No. UAC-2004-0052.

APPENDIX A: DERIVATION OF EQ. (7)

In the limit of small lattice spacing a the sums over the grid points n in eq. (6) can be approximated by integrals

over the quasi continuous variable $x = na$:

$$\sum_{n=-\infty}^{\infty} t(na) \exp[ikna] \approx \frac{1}{a} \int dx t(x) e^{ikx} \quad (A1)$$

and

$$\sum_{n=-\infty}^{\infty} s(na) \exp[ikna] \approx \frac{1}{a} \int dx s(x) e^{ikx}. \quad (A2)$$

Thus the two sums are approximately given by the Fourier transform of the hopping integral $t(x)$ and the overlap integral $s(x)$, respectively. Since the overlap integral is a Gaussian function, $s(x) = \exp[-\alpha x^2]$, its Fourier transform $\tilde{s}(k)$ is also simply a Gaussian:

$$\tilde{s}(k) = \frac{1}{\sqrt{2\pi}} \int dx s(x) e^{ikx} = \alpha^{-1/2} \exp[-k^2/2\alpha]. \quad (A3)$$

The Fourier transform $\tilde{t}(k)$ of the hopping integral $t(x) = \frac{\alpha}{2}(1 - \alpha x^2) \exp[-\alpha x^2]$ is a bit more involved:

$$\begin{aligned} \tilde{t}(k) &= \frac{1}{\sqrt{2\pi}} \int dx t(x) e^{ikx} \\ &= \frac{\alpha}{2} \tilde{s}(k) - \frac{\alpha^2}{2} \frac{1}{\sqrt{2\pi}} \int dx x^2 s(x) e^{ikx} \\ &= \frac{\sqrt{\alpha}}{2} \exp[-k^2/2\alpha] - i^2 \frac{\alpha^2}{2} \frac{d^2}{dk^2} \tilde{s}(k) \\ &= \left(\frac{\sqrt{\alpha}}{2} + \frac{\alpha^2}{2} \alpha^{-1/2} \left(-\frac{1}{\alpha} + \frac{k^2}{\alpha^2} \right) \right) \exp[-k^2/2\alpha] \\ &= \frac{k^2}{2} \alpha^{-1/2} \exp[-k^2/2\alpha]. \end{aligned} \quad (A4)$$

Thus, in total we obtain for the energy dispersion $\epsilon(k)$ in the limit of small a :

$$\epsilon(k) = \frac{\sum_n t(na) \exp[ikna]}{\sum_n s(na) \exp[ikna]} \approx \frac{\tilde{t}(k)}{\tilde{s}(k)} = \frac{k^2}{2}. \quad (A5)$$

This proves eq. (7) since in the limit $a \rightarrow 0$ the approximation of the sums by integrals becomes exact.

* Electronic address: dsh2@alu.ua.es

† Electronic address: djacob@physics.rutgers.edu

‡ Electronic address: jj.palacios@ua.es

¹ R. H. Fowler and L. W. Nordheim, Proc. R. Soc. London, Ser. A **119**, 173 (1928).

² W. A. de Heer, W. Bacsá, A. Châtelain, T. Gerfin, R. Humphrey-Baker, L. Forro, and D. Ugarte, Science **268**, 845 (1995).

³ J.-M. Bonard, J.-P. Salvetat, T. Stöckli, W. A. d. Heer, L. Forró, and A. Châtelain, Appl. Phys. Lett. **73**, 918 (1998).

⁴ J.-M. Bonard, K. A. Dean, B. F. Coll, and C. Klinke, Phys. Rev. Lett. **89**, 197602 (2002).

⁵ G. Collins and A. Zettl, Phys. Rev. B **55**, 9391 (1997).

⁶ S.-D. Liang, N. Y. Huang, L. Chen, S. Z. Deng, and N. S. Xu, Phys. Rev. B **73**, 245301 (2006).

- ⁷ S. Han and J. Ihm, Phys. Rev. B **61**, 9986 (2000).
- ⁸ C. Kim, B. Kim, S. M. Lee, C. Jo, and Y. H. Lee, Phys. Rev. B **65**, 165418 (2002).
- ⁹ C. Kim, K. Seo, B. Kim, N. Park, Y. S. Choi, K. A. Park, and Y. H. Lee, Phys. Rev. B **68**, 115403 (2003).
- ¹⁰ S. Han, M. H. Lee, and J. Ihm, Phys. Rev. B **65**, 085405 (2002).
- ¹¹ K. Tada and K. Watanabe, Phys. Rev. Lett. **88**, 127601 (2002).
- ¹² M. Di Ventura, S. T. Pantelides, and N. D. Lang, Phys. Rev. Lett. **84**, 979 (2000).
- ¹³ J. J. Palacios, A. J. Pérez-Jiménez, E. Louis, and J. A. Vergés, Phys. Rev. B **64**, 115411 (2001).
- ¹⁴ J. J. Palacios, A. J. Pérez-Jiménez, E. Louis, E. SanFabián, and J. A. Vergés, Phys. Rev. B **66**, 035322 (2002).
- ¹⁵ M. Brandbyge, J. L. Mozos, P. Ordejón, J. Taylor, and K. Stokbro, Phys. Rev. B **65**, 165401 (2002).
- ¹⁶ J. Taylor, H. Guo, and J. Wang, Phys. Rev. B **63**, 121104 (2001).
- ¹⁷ J. M. Blanco, C. González, P. Jelínek, J. Ortega, F. Flores, and R. Pérez, Phys. Rev. B **70**, 085405 (2004).
- ¹⁸ J. M. Beebe, B. Kim, J. W. Gadzuk, C. D. Frisbie, and J. G. Kushmerick, Phys. Rev. Lett. **97**, 026801 (2006).
- ¹⁹ D. Jacob and J. J. Palacios, Phys. Rev. B **73**, 075429 (2006).
- ²⁰ D. Jacob, Ph.D. thesis, Universidad de Alicante (2007), arXiv:0712.1383v1.
- ²¹ M. J. Frisch, G. W. Trucks, H. B. Schlegel, G. E. Scuseria, M. A. Robb, J. R. Cheeseman, J. A. Montgomery, Jr., T. Vreven, K. N. Kudin, et al., Gaussian 03, Revision B.01, Gaussian, Inc., Pittsburgh PA, 2003.
- ²² V. Saunders, R. Dovesi, C. Roetti, R. Orlando, C. Zicovich-Wilson, N. Harrison, K. Doll, B. Civalleri, I. J. Bush, P. D'arco, et al., CRYSTAL03, Release 1.0.2, Theoretical Chemistry Group - Universita' Di Torino - Torino (Italy).
- ²³ N. W. Ashcroft and N. D. Mermin, *Solid State Physics* (Harcourt College Publishers, Orlando, 1976).
- ²⁴ Alternatively, we could choose, e.g., the minimum of $m^*(k)$. However, this would result in only slightly lower values for k_{\max} since the minimum occurs immediately before the singularity of $m^*(k)$ as can be seen from Fig.2.
- ²⁵ E. N. Economou, *Green's functions in Quantum Physics*, no. 7 in Springer Series in Solid State Physics (Springer, Berlin-Heidelberg-New York-Tokyo, 1970).
- ²⁶ V. M. Vainberg, V. D. Mur, V. S. Popov, , and A. V. Sergeev, Pis'ma Zh. Eksp. Teor. Fiz. **44**, 9 (1986).